DYNAMIC CHARACTERISTICS OF SOILS IN YUAN-LIN LIQUEFACTION AREA

Tzou-Shin Ueng*, Meei-Ling Lin, I-Yin Li, Chien-Ming Chu, and Jia-Shien Lin
Department of Civil Engineering
National Taiwan University
Taipei, Taiwan 106, R.O.C.

Key Words: liquefaction, earthquake, dynamic characteristics, testing.

ABSTRACT

The Chi-Chi Earthquake induced extensive soil liquefaction in many areas in central Taiwan, and caused substantial damage to buildings, roadways, bridges, and water front structures. Field investigation and explorations were performed in Yuan-Lin and its neighboring towns, Da-Chun and Sheh-Tou. Thin-walled tube "undisturbed" soil samples were taken during the subsurface explorations. Laboratory dynamic tests were conducted on these samples collected by National Taiwan University and the National Center for Research on Earthquake Engineering. The liquefaction test results provide the relation between cyclic shear stress ratio and number of stress cycles to initial liquefaction. The stress-strain relations during the stress-controlled and strain-controlled cyclic triaxial tests, and resonant column test results were obtained to study the characteristics of shear modulus and damping of these soils at various strain amplitudes. The results can be used in seismic ground response analysis in the Yuan-Lin area. The stiffness reduction versus pore pressure generation under cyclic loading was also studied. The results can be used for the evaluation of the soil-structure interaction and the design of foundations under earthquake loading.

I. INTRODUCTION

The Chi-Chi Earthquake of September 21, 1999 is the largest and most damaging earthquake that has struck Taiwan in a century. With a magnitude of 7.3 (M_w=7.6), the earthquake induced ground shakings of very high intensities in central Taiwan. Among the most shocking phenomena during this earthquake were the great displacements of the fault ruptures and a large number of landslides induced by the ground shaking. At the same time, extensive soil liquefaction occurred in many areas during this earthquake and caused severe damage.

Figure 1 shows the reported soil liquefaction locations. The intensity contours of ground shaking are also shown on the same figure (NCREE, 1999). Among these locations, Yuan-Lin and towns in its vicinity, Wu-Feng, and Nan-Tou are the sites with the most widespread liquefaction and severe damage to buildings, levees, roadways, retaining walls, and other structures. Sinking as much as 2 m and tilting of up to 10° due to uneven settlement were the most common types of building damage. Many buildings suffered lateral displacements of more than 1 m. These affected buildings were often found structurally intact. Collapses of houses because of structural

*Correspondence addressee

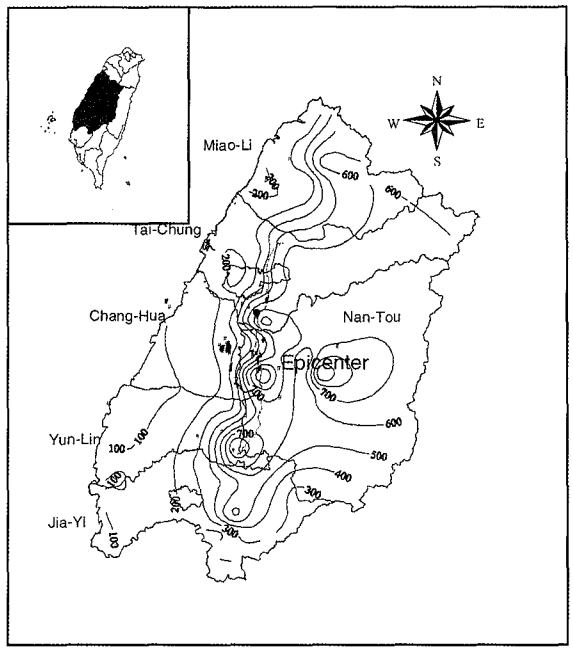

Fig. 1 The reported soil liquefaction locations and PGA contours

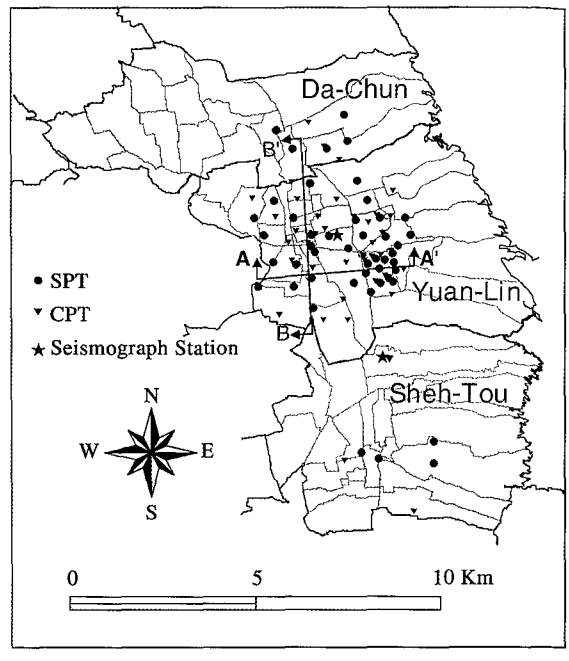

Fig. 2 Borehole locations for the investigation in the Yuan-Lin area

failures were rare in the liquefaction zones.

Moh and Associates, Inc. (MAA) also conducted field investigations and subsurface explorations for the National Science Council, ROC in Yuan-Lin, Wu-Feng and Nan-Tou (MAA, 2000). Standard penetration tests (SPT), cone penetration tests (CPT), and reflection, down-hole and cross-hole seismic wave velocity measurements were performed. Locations of boreholes and tests are shown in Fig. 2.

"Undisturbed" thin-walled tube and disturbed SPT soil samples were obtained during the subsurface explorations. The thin-walled tube samples taken from the sandy layers during the subsurface exploration were frozen after drainage of water, and kept frozen during transport, storage, tube cutting and test preparation until in the triaxial chamber, under a confining pressure. For the clayey soils, most of the samples were not frozen.

The Department of Civil Engineering, National Taiwan University and the National Center for Research on Earthquake Engineering (NCREE) collected most of the soil samples from Yuan-Lin and its neighboring towns, Da-Chun and Sheh-Tou, and conducted the laboratory dynamic tests including stress-controlled and strain-controlled cyclic triaxial tests using CKC dynamic triaxial test apparatus, resonant column tests using Stokoe (fixed-free) type torsion shear/resonant column tests apparatus, and bender element tests developed by the Norwegian Geotechnical Institute. In order to study the behavior of the soil after cyclic loading, static monotonic triaxial compression tests were performed on some specimens after the cyclic triaxial tests. Other properties such as unit weight, grain size, plasticity, etc. were also obtained for these samples. Details of the tests are given in Li (2001), Chu (2001), and Lin (2001). Table 1 lists the soil samples taken from the Yuan-Lin area and the laboratory dynamic tests performed on them.

This paper reports on the study of the dynamic characteristics, including shear wave velocity, liquefaction resistance, shear modulus, damping, and stiffness reduction versus pore water pressure generation under cyclic loading, of the soils in the Yuan-Lin liquefaction area. The properties are to be used for liquefaction evaluation, ground motion analysis, and foundation designs under earthquake loading in this area.

II. GEOLOGY AND SOIL PROFILES

Yuan-Lin is located about 30 km from the epicenter of the Chi-Chi Earthquake and 10 km west of the ruptured Chelungpu fault. Earthquake records at two seismograph stations within the study area were obtained. The peak ground accelerations were 188 gal and 207 gal at Yuan-Lin station and Sheh-Tou station, respectively (Fig. 3). The seismogram at Yuan-Lin station indicates a rather long shaking period during the Chi-Chi Earthquake.

The town of Yuan-Lin is situated on a thick alluvial deposit from the Tsoshui River in the foothills

Table 1 Dynamic tests on soil samples from the Yuan-Lin area

Sample No.	Depth (m)	Soil type	SPT-N	γ_d (kN/m^3)	Site liquefaction in earthquake	Tests performed	CSR	N_L
BH-3, T-2	3.25~4.00	SM	5	12.7	Y	CTS, RC	0.206	150
							0.273	34
BH-3, T-3	4.00~4.75	CL	5	12.0	Y	CTS, RC	0.283	–
BH-3, T-5	15.05~15.75	SM	13	13.7	Y	CTS	0.30*	9
BH-5, T-2	3.75~4.54	SM	5	13.3	Y	CTS, RC	0.299*	5
							0.27	24
							0.25	80
BH-5, T-4	8.00~8.71	CL	3	13.4	Y	CTS	0.205	–
BH-11, T-1	9.50~10.25	SM	4	13.8	Uncertain	CTS	0.284*	22
							0.20	218+
BH-11, T-3	14.55~15.30	SM	8	14.9	Uncertain	CTS	0.36	7
							0.34*	10
BH-11, T-4	15.30~16.02	SM	8	16.3	Uncertain	CTS	0.28	19
							0.30*	19
BH-11, T-5	16.02~16.77	SM	8	15.9	Uncertain	CTS	0.32*	18
BH-15, T-1	2.00~2.75	CL	7	13.1	N	CTS, CTN, RC, BE	0.224	–
BH-15, T-2	5.60~6.35	ML	3	13.5	N	RC	–	–
BH-15, T-6	14.00~14.75	CL	9	14.5	N	CTS, CTN, RC, BE	0.314	–
BH-15, T-8	22.60~23.35	ML	13	14.0	N	CTN, RC	–	–
BH-15, T-9	27.15~27.90	ML	17	14.8	N	RC	–	–
BH-15, T-10	30.50~31.25	CL	11	14.0	N	CTN, RC	–	–
BH-15, T-11	37.25~38.00	ML	25	13.6	N	CTN, RC	–	–
BH-15, T-12	40.50~41.25	CL/ML	19	16.2	N	CTN, BE	–	–
BH-15, T-13	45.50~46.25	ML	21	14.8	N	CTN, RC, BE	–	–
BH-15-1, T-1	6.50~7.25	ML	5	15.2	N	RC	–	–
BH-21-1, T-1	4.10~4.85	SM	9	14.6	Y	CTS	0.215	218+
							0.28	167
							0.315	55
BH-25, T-1	12.70~13.45	SM	8	15.6	Y	RC	–	–
BH-28, T-2	12.70~13.45	ML/SM	18	15.0	Y	CTS, RC	0.294*	7
BH-34, T-2	6.90~7.64	SM	9	15.0	Uncertain	CTS	0.25*	218+
							0.29	28
BH-34, T-4	15.00~15.75	SM	14	14.8	Uncertain	CTS	0.29	42
							0.30	18
BH-34, T-6	17.50~18.05	SM	27	17.3	Uncertain	CTS	0.29	7

Note: CTS = stress-controlled cyclic triaxial test; BE = bender element test
CTN = strain-controlled cyclic triaxial test; N_L = number of cycles to liquefaction for the sandy soil
RC = resonant column test; * = indicates equivalent CSR induced by the Chi-Chi earthquake

of Baguashan. The depth of the bedrock surface increases from east towards west, reaching a depth of more than 200 m, according to the exploration holes drilled by the Central Geological Survey. The typical soil profiles within the study area, based on the borehole data of the field investigation, are shown in Fig. 4. There exist layers of very loose sandy soils with SPT-N values as low as 2. The ground water level is generally high at about 0.5 m to 4.0 m below ground surface. The shear wave velocities of the soils are about 100 m/s near the surface, increasing to around 250 m/s at a depth of 30 m, and approximately 600 m/s at a depth of 100 m (MAA, 2000).

It can be seen that there is generally a thicker layer of clayey soils in the western part of Yuan-Lin and it becomes thinner towards the eastern side of

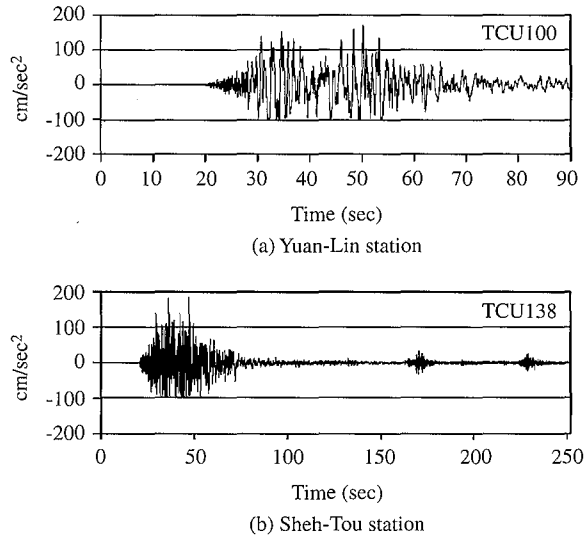

Fig. 3 N-S component of earthquake records for the seismograph stations in the Yuan-Lin area

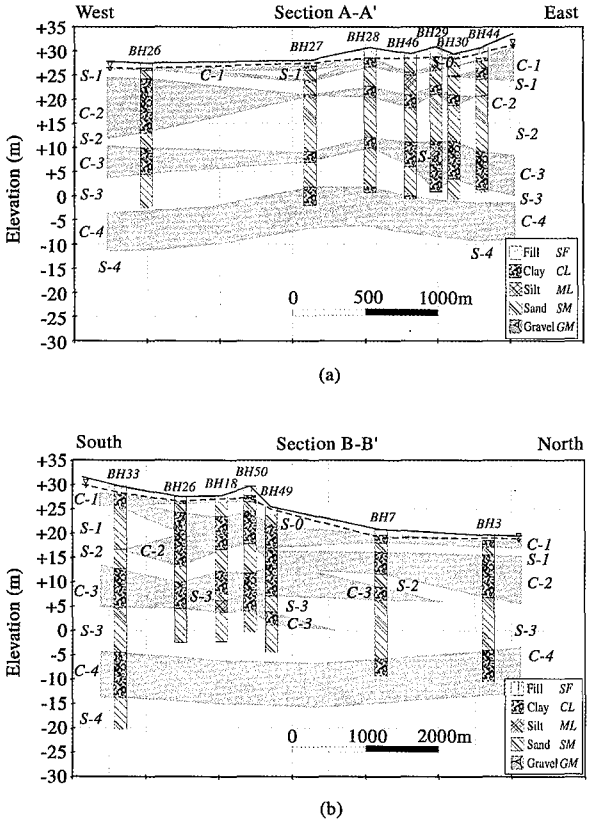

Fig. 4 Typical soil profiles in the Yuan-Lin area, (a) east-west section and (b) north-south section

the town. Some locations may even have a sand deposit at the ground surface without a clayey layer above it. It was found that liquefaction occurred in layers of sandy materials with low SPT-N values, usually less than 10. Sand boiling was not usually

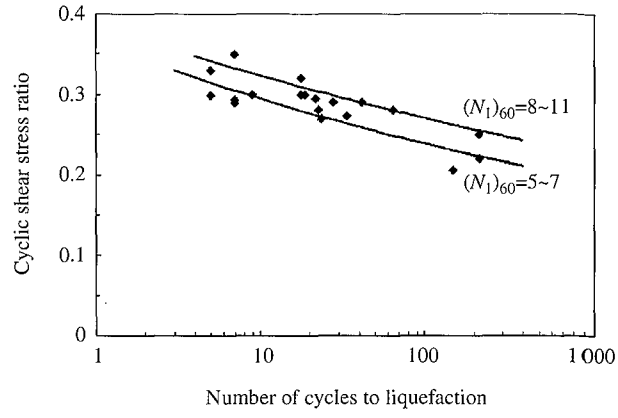

Fig. 5 Cyclic stress ratio versus number of cycles to liquefaction for sand in the Yuan-Lin area

observed in the areas with thick clay layers on top of the liquefiable sandy layers. Severe damage was found in ground with thin layers or completely missing layers of clay coverage. Some ground subsidence and tilting of buildings were also found in areas with a thick clay layer at the surface, probably due to the liquefaction of the underlying sandy layers or weakening of the clay during the earthquake.

The sandy soils obtained from the thin-walled tubes in this study were mostly silty fine sands with high fines contents of about 15%~45% and occasionally some coarse sand and gravels. The fine-grained materials ranged from low plastic clayey silt to silty clay of PI=8~17.

III. LIQUEFACTION TEST RESULTS

Stress-controlled cyclic (1 Hz) triaxial tests were performed on the sandy soils to obtain the liquefaction resistance. The test results gave the relation between cyclic shear stress ratio (i.e., $\frac{\sigma_d}{2\sigma_c'}$, where σ_d=cyclic deviator stress and σ_c'=effective confining pressure) and number of stress cycles causing initial liquefaction as shown in Fig. 5. The equivalent field cyclic stress ratio to induce liquefaction at a given number of stress cycles, or the cyclic resistance ratio (CRR) can be calculated using the results of the laboratory cyclic triaxial test according to the following relation:

$$CRR = \left[\frac{\tau_{av}}{\sigma_v'}\right]_{field} = 0.9C_r\left[\frac{\sigma_d}{2\sigma_c'}\right]_{triaxial} \quad (1)$$

in which C_r is a function of the overconsolidation ratio and coefficient of earth pressure at rest (Seed, 1979). Based on the test results, there is no good correlation between the liquefaction resistance and the corrected SPT-N values, $(N_1)_{60}$, of the soil layer of these tested specimens. Here, $(N_1)_{60}$ includes the corrections for

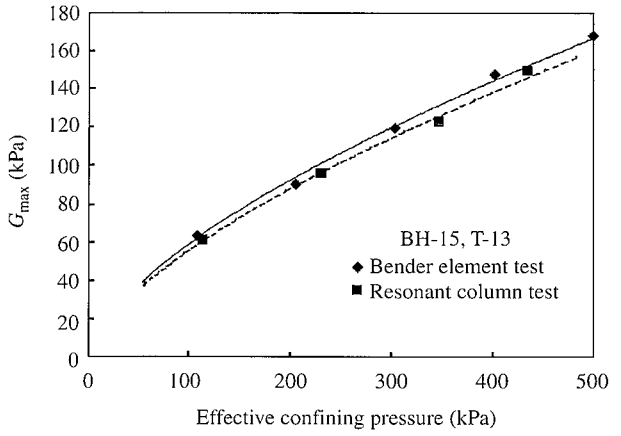

Fig. 6 Comparison of G_{max} between resonant column test and bender element test

effective overburden pressure, hammer energy, and rod length (Youd *et al.*, 2001). However, there is a general trend that the soil with a higher $(N_1)_{60}$ exhibits a higher liquefaction resistance. Judging from the laboratory and field data, rough approximate relations of liquefaction resistances for two different ranges of $(N_1)_{60}$ (5~7 and 8~11) are given in Fig. 5.

The cyclic shear stress ratio (CSR) on the soil induced by the earthquake shaking can be calculated according to Seed's method of soil liquefaction potential evaluation (Seed, *et al.*, 1985):

$$CSR = \frac{\tau_{av}}{\sigma_v'} = 0.65 \cdot \left[\frac{a_{\max}}{g}\right]\left[\frac{\sigma_v}{\sigma_v'}\right] \cdot r_d \qquad (2)$$

where τ_{av}=equivalent average cyclic shear stress on the soil,

$a_{\max}$ =peak ground acceleration, the measured value of 0.19 g at Yuan-Lin during the Chi-Chi Earthquake is used in this study,
g =acceleration of gravity,
σ_v =total vertical stress,
σ_v' =effective vertical stress,
r_d =stress reduction factor considering flexibility of the soil (Youd *et al.*, 2001).

The equivalent number of cycles of shaking induced by the Chi-Chi Earthquake (M_w=7.6) is about 15~20 according to Youd *et al.* (2001) and Hwang *et al.* (2000). The values of CRR and CSR of a soil sample can be calculated and compared to evaluate whether liquefaction could have possibly occurred during the Chi-Chi Earthquake. The available test results listed in Table 1 indicate that those samples from the soil strata within which liquefaction probably occurred during the Chi-Chi Earthquake liquefied under the equivalent cyclic loading in the cyclic triaxial tests.

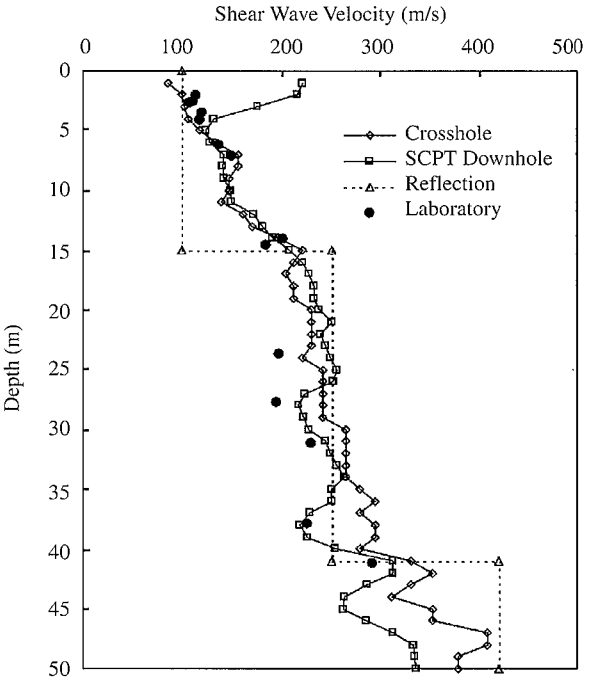

Fig. 7 Shear wave velocities at BH-15

IV. SHEAR WAVE VELOCITIES AND G_{max}

Resonant column tests were performed to obtain the modulus and damping for small strains from less than 10^{-4}% to about 2×10^{-3}%. The shear modulus increased with decreasing strain and reached a maximum value (G_{max}) at a strain less than 10^{-4}%. Bender element tests on four soil samples were conducted to obtain the shear wave velocity, and in turn, the maximum shear modulus (G_{max}) at a very low strain level (Dyvik and Madshus, 1985). The results, as shown in Fig. 6, indicated that there is only a very slight difference of G_{max} obtained in these two methods. The values of G_{max} obtained in the resonant column tests were used in this study.

Shear wave velocities of the soils in the Yuan-Lin area were measured during the field investigation by MAA. The measurements included surface reflections, down-hole seismic wave velocity measurements in CPT, and cross-hole seismic tests between two boreholes. Fig. 7 shows that the shear wave velocities of soils in Yuan-Lin obtained by these three methods are comparable with slightly lower values by the down-hole method at depths below 30 m. The field shear wave velocity generally increases with the effective vertical stress at site (Fig. 8). It also varies with $(N_1)_{60}$ value (or relative density) with scattering as shown in Fig. 9.

Field wave velocities were generally measured under a very small strain, less than 10^{-4}%. Therefore, the value of shear modulus, G, calculated from the

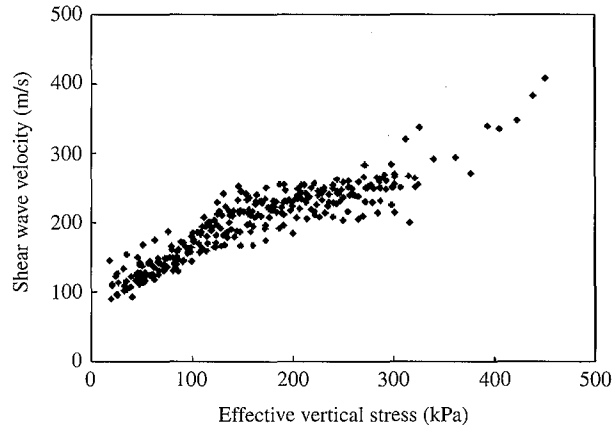

Fig. 8 Field shear wave velocities versus effective vertical stresses

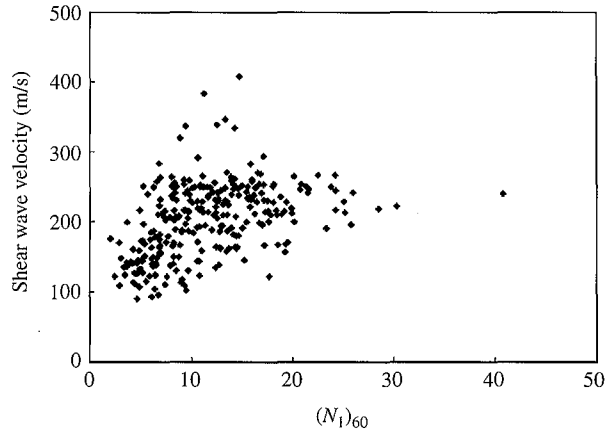

Fig. 9 Field shear wave velocities versus corrected SPT-N values

field measured shear wave velocity, V_s, i.e., $G=\rho V_s^2$, can be considered as G_{max}, where ρ is the density of the soil. Conversely, shear wave velocity can be computed using G of the soil. Since a uniform confining pressure is applied on the specimen in the laboratory test, which differs from the field geostatic stress (K_o) condition, the computations of field shear wave velocities from G_{max} obtained in the laboratory should be corrected according to the effective mean stress (σ'_m). Shear wave velocities computed from G_{max} obtained in the resonant column tests for samples from Borehole BH-15 at the Yuan-Lin seismograph station are compared with the field measurements. Fig. 7 shows a rather good agreement even though the soil samples tested in the laboratory are commonly disturbed and usually give smaller wave velocities than those measured in the field.

G_{max} values calculated from the field measured shear wave velocity in the Yuan-Lin area, are similarly affected by both SPT-N value and effective mean stress (σ'_m) at the site. Eqs. (3a) and (3b) are the regression correlations based on these calculated G_{max}

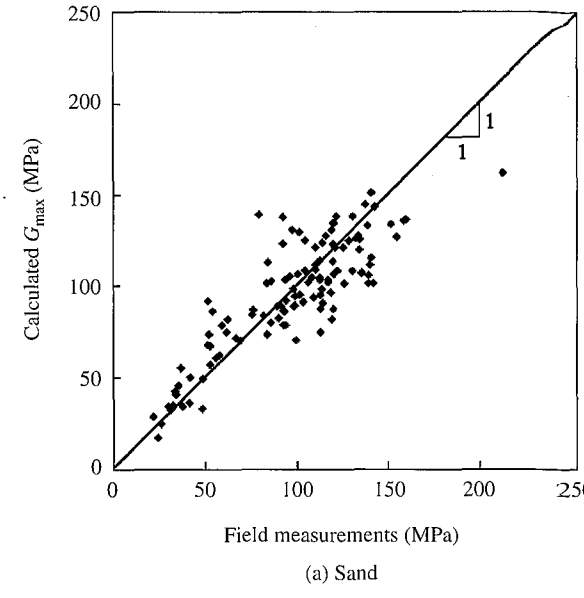

(a) Sand

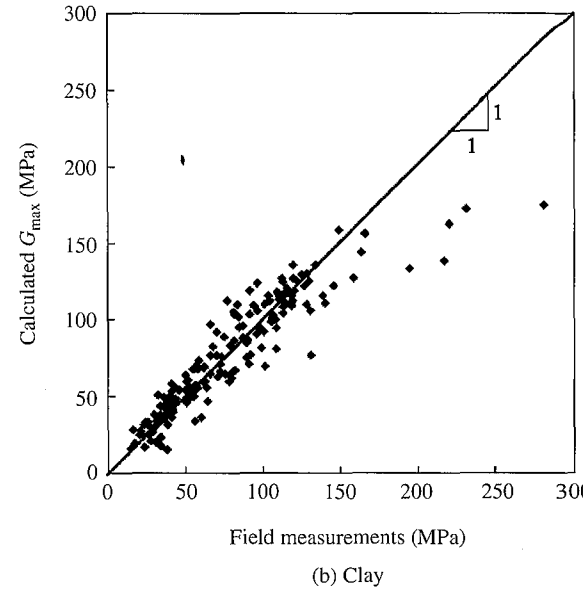

(b) Clay

Fig. 10 Comparison of G_{max} obtained from field measured wave velocities and those calculated from Eq. (3)

values assuming K_o=0.5:

$$\text{Sand: } G_{max}(\text{kPa})=2465((N_1)_{60})^{0.186}(\sigma'_m)^{0.659},\quad R^2=0.733 \tag{3a}$$

$$\text{Clay: } G_{max}(\text{kPa})=2190((N_1)_{60})^{0.067}(\sigma'_m)^{0.743},\quad R^2=0.812 \tag{3b}$$

Figure 10 shows the comparisons of G_{max} values obtained from the field wave velocity measurements and those calculated according to Eq. (3) for sand and clay in the Yuan-Lin area. The relations are reasonably good for soils with shear moduli less

than about 200 MPa. More data are needed to obtain better correlations for soils with higher moduli at a greater depth (> 40m).

V. SHEAR MODULUS AND DAMPING

The shear stress-strain relations in the stress-controlled cyclic triaxial tests (liquefaction tests) were recorded and the dynamic shear modulus and damping for each stress cycle were obtained based on the stress-strain relation. Since shear strains in the stress-controlled liquefaction tests are usually large initially (mostly > 0.1%) and progressive to failure without control, strain-controlled cyclic triaxial tests were conducted for the shear modulus and damping of the soil at a given strain amplitude as low as about 10^{-2}%. Due to the limitations of our equipment, the cyclic period in the strain-controlled tests was 120 s~180 s. The shear modulus and damping of soil in the triaxial tests were calculated according to the secant modulus connecting two peak points, and the area of the hysteresis loop, respectively, of the stress-strain relation in a stress cycle (ASTM D 3999-91, 2000).

Combining the test results from resonant column tests and cyclic triaxial tests, Fig. 11 shows the results of shear modulus versus shear strain amplitude (G/G_{max} vs. γ) for sand and clay in the Yuan-Lin area. The shear modulus is normalized against G_{max} of the soils. G_{max} can be obtained in the resonant column tests or calculated from the shear wave velocity measured nearby. For some samples in the cyclic triaxial tests without resonant column tests or wave velocity measurements of the same soil, G_{max} values were computed using Eq. (3) according to the field effective stresses and SPT-N values of the same soil strata.

According to Fig. 11, the G/G_{max} versus γ relation of sandy soils in the Yuan-Lin area lies between the relations for PI=0 and PI=30 given by Vucetic and Dobry (1991). The curve of PI=0 by Vucetic and Dobry (1991) is the mean value for clean sands given by Seed and Idriss (1970). At small shear strains, the mean value of the relationship in the Yuan-Lin area is about that of PI=15 by Vucetic and Dobry, while for shear strains γ>0.2%, the mean value matches Vucetic and Dobry's PI=0 relation. This type of relationship may result from the high content (>15%) of non-plastic fines in the sandy soils in the Yuan-Lin area. For clay and silt in the Yuan-Lin area, the G/G_{max} versus γ relation at γ<0.1% falls between the curves for PI=15 and PI=30 given by Vucetic and Dobry (1991) but between the relations for PI=0 and PI=15 for γ>0.1%.

The relations of damping ratio versus shear strain amplitude of the soils in the Yuan-Lin area are shown in Fig. 12. The results are more scattered than

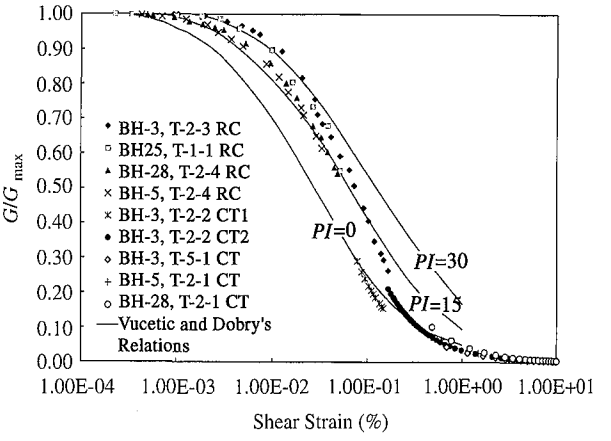

(a) Dand

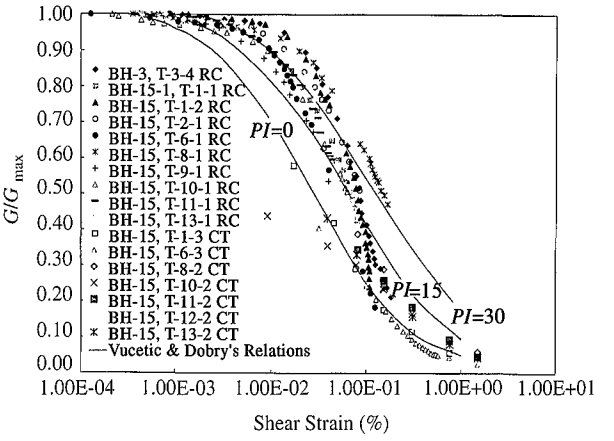

(b) Clay

Fig. 11 Relations of G/G_{max} versus shear strain for soils in the Yuan-Lin area

those for G/G_{max}, especially at higher strains. For both sand and clay, the damping ratios are near the minimum value of about 1% to 2% at γ<10^{-2}% and increase rapidly for γ>10^{-2}%. The relationship obtained in the Yuan-Lin area is slightly different from that by Vucetic and Dobry (1991), and Seed and Idriss (1970). The values of damping ratios are generally lower at low strains below 10^{-2}% and higher at higher strains.

VI. STIFFNESS REDUCTION VERSUS PORE PRESSURE GENERATION

During the cyclic triaxial tests, the dynamic modulus and the corresponding pore water pressure in each stress cycle were recorded. The variation of modulus was studied against the change of effective stress, or the ratio of pore water pressure increment to the original effective confining pressure, i.e., $r_u=\Delta u/\sigma_c'$. The ratio of shear modulus at various r_u to that at the first stress cycle (i.e., r_u=0), G/G_o, is used to study the stiffness reduction of soils under

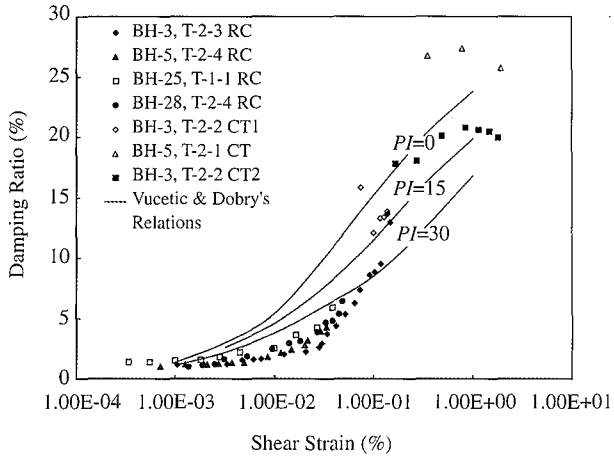

(a) Sand

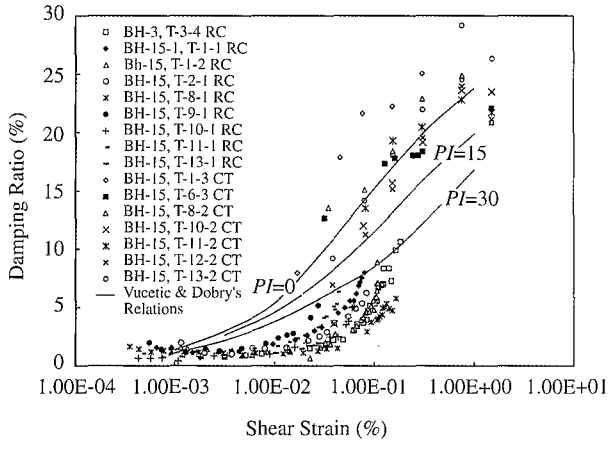

(b) Clay

Fig. 12 Relations of damping ratio versus shear strain for soils in the Yuan-Lin area

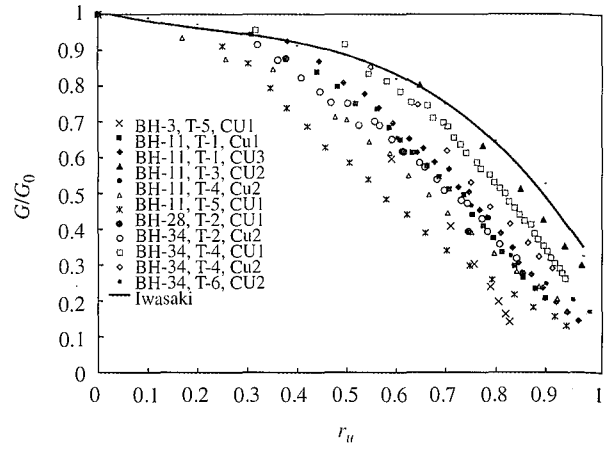

(a) Sand

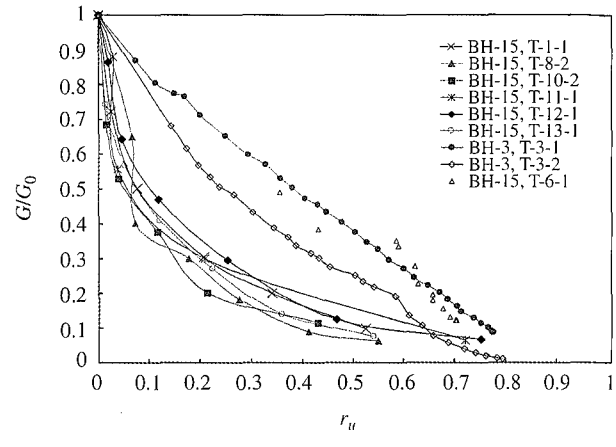

(b) Clay

Fig. 13 Shear modulus reduction versus pore pressure ratio for soils in the Yuan-Lin area

earthquake loading. The pore pressure at the mid-point of the maximum and minimum shear strains of a stress cycle is generally the highest pore pressure in the following stress cycle, and it is used for computation of r_u for the stress cycle. The trends of stiffness reduction are different between sand and clay in the Yuan-Lin area. For sand, as shown in Fig. 13a, there is a smaller stiffness reduction at the beginning of pore water pressure excitation, while the stiffness reduces more rapidly after $r_u \geq 0.6$. Stiffness reaches almost zero when the soil approaches initial liquefaction, i.e., $r_u=1.0$. The amount of stiffness reduction is affected by shear stress ratio, relative density, and fines content of the sand. The relation of stiffness reduction given by Iwasaki, *et al.* (1982) is also shown in Fig. 13a. Generally, the stiffness reduces more for sand in the Yuan-Lin area than the reductions obtained by Iwasaki, *et al.* (1982). This may be because the generation of the pore pressure in Iwasaki's study was induced by increasing the back pressure, while, in this study, the pore pressure was generated by cyclic loading which better simulates the pore water pressure changes under earthquake loading.

The stiffness of clay reduces more rapidly when the pore water pressure increases, and the rate of stiffness reduction decreases at higher r_u as shown in Fig. 13b. The stiffness can be quite low even for a moderate increase of pore pressure. This may explain the large settlements of buildings on the clayey soils without apparent liquefaction. The factors influencing the stiffness reduction of clay may include effective stress reduction, soil structure and sensitivity, plasticity, loading rate, etc. Details of these effects are not completely understood yet; more studies and testing in the field and the laboratory are needed to evaluate the stiffness reduction of clay under earthquake loading. The stiffness reduction of clay is affected also by the sandy interlayers. The trend of stiffness reduction is more like that of sand for clay

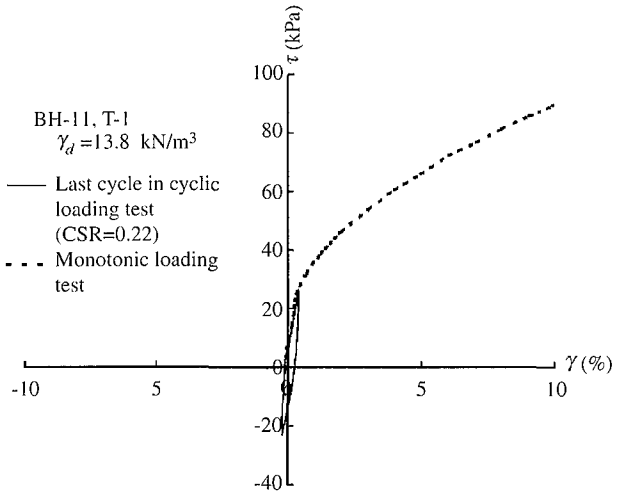

Fig. 14 Comparison of stress-strain relation (small strain) in cyclic loading and that in monotonic loading thereafter

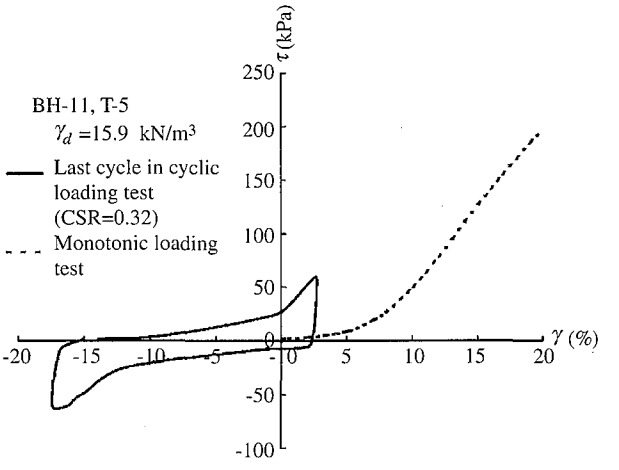

Fig. 15 Comparison of stress-strain relation for liquefied sand in cyclic loading and that in monotonic loading thereafter

interbedded with sandy layers.

Monotonic undrained compression tests were also performed on some specimens right after cyclic triaxial tests were terminated, either before or after the initial liquefaction. The strain-stress relations obtained in these tests were studied for more understanding of the interaction between the foundation and the soil during and after earthquakes. Figs. 14 and 15 show that, right after the cyclic loading, the monotonic loading stress-strain relations follow those in the last loading cycle. The results indicate that the initial shear modulus is essentially zero for soil that has reached liquefaction, and then the stiffness gradually increases as the strain increases. The stiffness increases significantly after shear strain reaches about 5% when the dilation of sand occurs. If the soil does not reach liquefaction, there is some stiffness in the soil to resist deformation. This is similar to findings by Vaid and Thomas (1995) and Jiang (2000). This should be taken into account for foundation design under earthquake loading.

VII. CONCLUSIONS

The 1999 Chi-Chi, Taiwan Earthquake induced very high shaking intensities in many areas in central Taiwan and caused extensive soil liquefaction. Soil liquefaction occurred in the town of Yuan-Lin and its vicinity and caused severe damage. Dynamic soil property tests were conducted on "undisturbed" thin-walled tube samples. The liquefaction resistance of the sandy soils in the Yuan-Lin area was obtained in terms of the relation between cyclic shear stress ratio and number of stress cycles to initial liquefaction. The results are used to evaluate the liquefaction conditions during the Chi-Chi Earthquake. The stress-strain relations during the stress-controlled and strain-controlled cyclic triaxial tests, and the results of the resonant column tests were used to obtain the shear modulus and damping of these soils at various strain amplitudes. The shear wave velocities computed from the modulus at very low strains in the laboratory tests compare well with the field measurements. The results can be used in seismic ground response analysis of the Yuan-Lin area. The trends of stiffness reductions under cyclic loading versus the pore water pressure ratio, r_u, of the sand and clay in the Yuan-Lin area are different. A more rapid stiffness reduction for clay than sand was found according to the test results.

NOMENCLATURE

a_{max}	peak ground acceleration (m/s²)
CRR	cyclic resistance ratio
CSR	cyclic shear stress ratio
$(N_1)_{60}$	SPT-N values with corrections for effective stress, energy and rod length
G	shear modulus (kPa)
G_{max}	maximum shear modulus at low shear strains (kPa)
G_o	shear modulus at first stress cycle (kPa)
g	the acceleration of gravity = 9.81 m/s²
PI	plasticity index
r_d	a stress reduction factor considering deformation of the soil
r_u	pore water pressure ratio=$\Delta u/\sigma_c'$
V_s	shear wave velocity (m/s)
Δu	pore water pressure increment (kPa)
γ	shear strain

ρ soil density (kg/m^3)
σ'_c effective confining pressure (kPa)
σ_d cyclic deviator stress (kPa)
σ'_m effective mean stress (kPa)
σ_v total vertical stress (kPa)
σ'_v vertical effective stress (kPa)
τ_{av} equivalent average cyclic shear stress on the soil (kPa)

ACKNOWLEDGEMENTS

This study was partly supported by the National Science Council, ROC, Grant Nos. NSC89-2211-E-002-151 and NSC89-2921-Z-319-005-17.

REFERENCES

1. ASTM, D 3999-91, 2000, "Standard Test Methods for the Determination of the Modulus and Damping Properties of Soils Using the Cyclic Triaxial Apparatus," *Annual Book of ASTM Standards*, Vol. 04.08.
2. Chu, C. M., 2001, "Using Shear Wave Velocity to Analyze Soil Liquefaction and Seismic Ground Response in the Yuan-Lin Areas," Master Thesis, Department of Civil Engineering, National Taiwan University, Taipei, Taiwan (in Chinese).
3. Dyvik, R., and Madshus, C., 1985, "Lab Measurements of G_{max} Using Bender Elements," *Advances in the Art of Testing Soils under Cyclic Conditions*, ASCE, pp. 186-196.
4. Hwang, J. H., Yang, C. W., Tan, C. H., and Chen, C. H., 2000, "Investigation on Soil Liquefactions During the Chi-Chi Earthquake," *Sino-Geotechnics*, No. 77, pp. 51-64.
5. Iwasaki, T., Aralawa, T., and Tokida, K., 1982, "Simplified Procedures for Assessing Soil Liquefaction During Earthquakes," *Soil Dynamics and Earthquake Engineering Conference*, Southampton, UK, pp. 925-939.
6. Jiang, K. L., 2000, "Undrained Shear Behavior of Saturated Sand after Cyclic Loading," *Master Thesis*, Department of Civil Engineering, National Taiwan University, Taipei, Taiwan (in Chinese).
7. Li, I. Y., 2001, " Dynamic Properties of Soils in the Yuan-Lin Area," *Master Thesis*, Department of Civil Engineering, National Taiwan University, Taipei, Taiwan (in Chinese).
8. Lin, J. S., 2001, "Soil Stiffness Reduction under Cyclic Loading for Soils in the Yuan-Lin Area," *Master Thesis*, Department of Civil Engineering, National Taiwan University, Taipei, Taiwan, (in Chinese).
9. MAA, 2000, *Soil Liquefaction Evaluation and Mitigation Study, Phase I (Yuen-Lin, Da-Chun and Sheh-Tou)*, Final Report to National Science Council, April 2000.
10. NCREE, 1999, *Reconnaissance Report of the Geotechnical Hazards Caused by Chi-Chi Earthquake*, National Center for Research on Earthquake Engineering, Taipei, Taiwan.
11. Seed, H. B., and Idriss, I. M., 1970, "Soil Modulus and Damping Factors for Dynamic Response Analysis," *EERC Report No. EERC 70-10, Earthquake Engineering Research Center*, University of California, Berkeley, CA, USA.
12. Seed, H. B., 1979, "Soil Liquefaction and Cyclic Mobility Evaluation for Level Ground during Earthquakes," *Journal of Geotechnical Engineering Division*, ASCE, Vol. 105, No. GT2, pp. 201-255.
13. Seed, H. B., Tokimatsu, K., Harder, L. F., and Chung, R. M., 1985, "Influence of SPT Procedures in Soil Liquefaction Resistance Evaluation," *Journal of Geotechnical Engineering Division*, ASCE, Vol. 111, No. 12, pp. 1425-1445.
14. Vaid, Y. P., and Thomas, J., 1995, "Liquefaction and Postliquefaction Behavior of Sand," *Journal of the Geotechnical Engineering*, ASCE, Vol. 121, No. 2, pp. 163-173.
15. Vucetic, M., and Dobry, R., 1991, "Effect of Soil Plasticity on Cyclic Response," *Journal of the Geotechnical Engineering*, ASCE, Vol. 117, No. 1, pp. 88-107.
16. Youd, T. L., Idriss, I. M., Andrus, R. D., Arango, I., Castro, G., Christian, J. T., Dobry, R., Finn, W. D. L., Harder, L. F., Hynes, M. E., Ishihara, K., Koester, J. P., Liao, S. S. C., Marcuson, W. F., Martin, G. R., Mitchell, J. K., Morwaki, Y., Power, M. S., Robertson, P. K., Seed, R. B., and Stokoe, K. H., 2001, "Liquefaction Resistance of Soils: Summary Report from the 1996 NCEER and 1998 NCEER/NSF Workshops on Evaluation of Liquefaction Resistance of Soils," *Journal of the Geotechnical and Geoenvironmental Engineering*, ASCE, Vol. 127, No. 10, pp. 817-833.

Manuscript Received: Aug. 20, 2001
Revision Received: Jan. 03, 2002
and Accepted: Jan. 28, 2002

員林液化地區土壤之動態特性

翁作新　林美聆　李怡穎　邱建銘　林家賢

國立台灣大學土木工程學系

摘　要

集集大地震引致彰化縣員林鎮及其相鄰地區之土壤液化災害及相關損壞相當嚴重。在此地區鑽探調查中取“不擾動”薄管土樣進行室內土壤動態特性之試驗與分析。從液化試驗得到不同反復剪應力比作用下，引致液化所需之反復荷重次數。由應力控制與應變控制之動力三軸試驗結果，配合共振柱試驗結果，得在不同應變振幅時員林地區土壤之動態剪力模數與阻尼比。反復作用力下土壤勁度之折減亦加以探討。本文資料可被引用爲探討員林地區土壤液化、受震地盤反應及基礎耐震設計之依據。

關鍵詞：液化，地震，動態特性，試驗。